NASA TECHNICAL NOTE

NASA TN D-4379

NASA TN D-4379

EFFECTS OF COMPOSITION AND HEAT TREATMENT ON HIGH-TEMPERATURE STRENGTH OF ARC-MELTED TUNGSTEN-HAFNIUM-CARBON ALLOYS

by L. S. Rubenstein

Lewis Research Center
Cleveland, Ohio

NATIONAL AERONAUTICS AND SPACE ADMINISTRATION • WASHINGTON, D. C. • FEBRUARY 1968

NASA TN D-4379

EFFECTS OF COMPOSITION AND HEAT TREATMENT ON HIGH-TEMPERATURE STRENGTH OF ARC-MELTED TUNGSTEN-HAFNIUM-CARBON ALLOYS

By L. S. Rubenstein

Lewis Research Center
Cleveland, Ohio

NATIONAL AERONAUTICS AND SPACE ADMINISTRATION

**For sale by the Clearinghouse for Federal Scientific and Technical Information
Springfield, Virginia 22151 – CFSTI price $3.00**

EFFECTS OF COMPOSITION AND HEAT TREATMENT ON HIGH-TEMPERATURE STRENGTH OF ARC-MELTED TUNGSTEN-HAFNIUM-CARBON ALLOYS

by L. S. Rubenstein

Lewis Research Center

SUMMARY

The effects of composition, heat treatments, and substructure on the strength and ductility of tungsten-hafnium-carbon (W-Hf-C) alloys were studied. The compositions ranged from 0.23 to 1.76 atomic percent for hafnium and from 0.179 to 0.942 atomic percent for carbon, with carbon to hafnium ratios from 0.17 to 2.80 and calculated amounts of hafnium carbide ranging up to 1.5 volume percent. The high-temperature tensile strengths of swaged, recrystallized, solution-annealed and aged alloys increased with increasing hafnium carbide contents up to approximately 0.5 volume percent, after which further additions caused a slight decrease in strength. The strongest alloys contained equiatomic amounts of carbon and hafnium. The 3500° F (2200° K) tensile strength for swaged material was linearly related to the inverse square root of the cell size.

Limited tensile and microstructural studies indicated that the W-Hf-C alloys are heat treatable. The minimum solution temperature of hafnium carbide in tungsten is approximately 4600° F (2810° K), and 1 hour at 2500° F (1644° K) is an effective aging temperature. A tensile specimen heat treated in this manner displayed a tensile strength of 69 000 psi (475×10^{6} N/m^{2}) at 3500° F (2200° K) compared to approximately 9000 psi (62×10^{6} N/m^{2}) for unalloyed tungsten. The hafnium carbide precipitation-strengthened alloys exhibited 1-hour recrystallization temperatures in excess of 4200° F (2589° K).

The stress for a 3500° F (2200° K), 100-hour rupture life was approximately 14 000 psi (96.5×10^{6} N/m^{2}) in the swaged condition. A solution-annealed and aged specimen tested in 3500° F (2200° K) step-load creep tests required a stress of approximately 20 000 psi (138×10^{6} N/m^{2}) for a minimum creep rate of 6×10^{-7} sec^{-1}, corresponding to an approximate 100-hour rupture life.

These W-Hf-C alloys exhibit a sevenfold strength improvement over unalloyed tungsten at 3500° F (2200° K) that is related to the precipitate stabilized, fine dislocation structure formed within the cell boundaries. For high-strength applications at 3500° F (2200° K), compositions composed of equiatomic amounts of carbon and hafnium, approximately 0.3 to 0.4 atomic percent, are recommended.

INTRODUCTION

The high melting point and elastic modulus of tungsten are the bases for considering tungsten base alloys for high-strength, high-temperature applications. An effort to develop arc-melted tungsten base alloys with good high-temperature strength and room-temperature ductility has been underway at Lewis for several years (refs. 1 to 3).

It was recently shown that carbon additions to dilute binary alloys of tungsten with tantalum, hafnium, columbium, and rhenium produced different degrees of strengthening with the highest strengths observed in the W-Hf-C system (ref. 4). Similar results were found by others for powder metallurgy tungsten alloys (ref. 5) and arc-melted tungsten base alloys (ref. 6). This report presents the results of a study to determine the effects of composition and heat treatment on the elevated temperature tensile and creep rupture properties, recrystallization temperatures, and substructures of W-Hf-C alloys.

Examination of the respective binary phase diagrams of the tungsten-carbon and tungsten-hafnium systems indicated that at 4535° F (2773° K) the solubility of carbon in tungsten is 0.3 percent, and of hafnium in tungsten is 15.5 percent. (Composition will be given in atomic percent, except where otherwise indicated.) At 1832° F (1273° K) the solubility of carbon in tungsten decreases to a negligible amount (ref. 7) and the solubility of hafnium in tungsten decreases to approximately 4 percent (ref. 8). The free energies of formation of hafnium carbide and tungsten carbide indicate that in the temperature range of interest, 1500° to 4000° F (1089° to 2478° K), hafnium carbide is more stable than tungsten carbide. Thus, the necessary conditions for precipitation of hafnium carbide exists in this alloy system and it was possible to design the experiment to obtain different amounts of this precipitate.

The compositions studied ranged from 0.23 percent hafnium to 1.76 percent hafnium, and from 0.179 percent carbon to 0.942 percent carbon, with carbon to hafnium ratios from 0.17 to 2.80, and calculated amounts of hafnium carbide ranging up to 1.5 volume percent. These compositions thus included alloys which contained hafnium carbide with excess hafnium in solution, and alloys which contained hafnium carbide plus carbon in solution, and as tungsten carbide.

EXPERIMENTAL PROCEDURE

The alloys were prepared by vacuum consumable, deep mold, arc-melting of 10-pound ingots from hydrostatically pressed and sintered electrodes made from high-purity elemental tungsten, hafnium, and carbon powders. The electrodes were sintered in vacuum for 4 hours at 4000° F (2478° K). The arc-melting furnace has beenpreviausly

TABLE I - ANALYSES OF ARC-MELTED AND

Ingot	Analyzed composition, at. %	Interstitial content, ppm by weight		
		Nitrogen	Oxygen	Hydrogen
A194	W-0.23Hf-0.21C		4	<1
A156	W-0.26Hf-0.68C		12	--
A218	W-0.31Hf-0.87C		5	--
A192	W-0.44Hf-0.18C	<5	4	<1
A193	W-0.48Hf-0.50C		12	--
A191	W-0.91Hf-0.94C	<5	10	<1
A190	W-1.68Hf-0.28C	<5	12	--
A174	W-1.76Hf-0.72C	<5	23	--

described in reference 1. The compositions of the ingots melted are given in table I.

Tensile tests and constant-load and step-load creep tests were conducted as described in references 2 and 3. Specimens for tensile and creep studies were ground from swaged rod with 1.03 inch (2.62×10^{-2} m) long reduced sections and diameters ranging from 0.125 (0.317×10^{-2} m) to 0.160 inch (0.406×10^{-2} m). Tensile tests were performed in vacuum at 1×10^{-5} torr (1.33×10^{-3} N/m^2) with a constant crosshead speed of 0.05 inch per minute (2.08×10^{-5} m/sec). The specimens were brought to the test temperature in approximately 1 hour and held at temperature for 5 minutes prior to testing.

Creep tests were conducted in a conventional beam-loaded machine equipped with a vacuum chamber and tantalum heater. Pressure during testing was maintained at 1×10^{-6} torr (1.33×10^{-4} N/m^2) or less. Specimen extensions were measured from loading rod movement.

Tensile and creep specimen temperatures were measured during testing with calibrated tungsten - tungsten 26 percent rhenium thermocouples tied to the center of the specimen reduced section. Grain sizes were measured in the heated but undeformed shoulders of all tensile and creep specimens after testing.

The cast billets were machined to size, canned in molybdenum, induction heated in hydrogen to 4000° F (2478° K), and extruded to rod in a conventional hydraulic press at a reduction ratio of 8 to 1. The molybdenum cladding was retained for swaging, which was conducted in the temperature range of 3500° to 3200° F (2200° to 2033° K) with reductions of approximately 10 to 15 percent per pass to total reductions of approximately 83 to 85 percent. Portions of the molybdenum clad extrusions were also flat rolled to sheet at starting temperatures of 3250° F (2061° K) and at finishing temperatures 100° F lower. The final rolling pass was accomplished after chemical removal of the molybdenum and surface conditioning by grinding.

Annealing treatments at temperatures up to 3400° F (2144° K) were conducted in an induction furnace with a hydrogen atmosphere, while treatments from 3500° to 5000° F (2200° to 3030° K) were conducted in a water-cooled stainless-steel vacuum (1×10^{-5} torr (1.33×10^{-3} N/m^2)) furnace chamber equipped with a tungsten mesh heating element.

Specimens for light microscopy were either mechanically or electrolytically polished. The etchant employed was boiling 3 percent hydrogen peroxide. Electron transmission studies were conducted on disks spark-machined from the reduced sections of creep and tensile specimens after testing. These were thinned using an electrolyte of 3 percent sodium hydroxide as described in reference 9. Selected area diffraction was also employed to identify particles obtained by an extraction replica technique. In general, the dislocation substructure of the swaged material consisted of a cellular structure. The cell size was measured on electron micrographs by the line intercept method using a circle to achieve randomness.

RESULTS

High-Temperature Tensile Testing of Swaged and Recrystallized Material

The elevated temperature tensile strengths of the W-Hf-C alloys depend on the heat treatment and processing history, the alloy composition, the precipitate content, and the amount and kind of substructure formed during deformation. Table 11 presents the tensile test results for the swaged and recrystallized W-Hf-C alloys. Included in this table are the carbon to hafnium ratios (in atomic percent) and calculated hafnium carbide contents of the ingots. The volume percent hafnium carbide was calculated by assuming stoichiometric hafnium carbide and using the chemical composition of the swaged rod, for either hafnium or carbon, whichever is lower in amount. Figure 1 shows that as the volume percent precipitate increases, a rapid increase in the 3500° F (2200° K) tensile strength occurs up to approximately 0.5 volume percent hafnium carbide, after which further additions cause a decrease in tensile strength. Figure 2 shows the effect of test temperature and hafnium carbide content on the tensile strength of the recrystallized material. At both 3000° F (1922° K) and 3500° F (2200° K), the tensile strength decreases with higher precipitate contents greater than 0.5 to 0.8 volume percent; however, the 2500° F (1644° K) tensile strength is relatively insensitive to hafnium carbide contents in amounts greater than 0.5 volume percent. It is also seen that, for material with hafnium carbide contents of 0.4 to 0.8 volume percent, the strengths at 3000° F (1922° K) are somewhat higher than at 2500° F (1644° K). Figure 3 shows that the 3500° F (2200° K) tensile strength increases, at a given hafnium content, with increasing carbon

TABLE II. - HIGH-TEMPERATURE TENSILE PROPERTIES OF W-Hf-C ALLOYS

Ingot	Composition, at. %	Carbon to hafnium ratio, at. %	Calculated hafnium carbide, vol. %	0.2-Percent yield strength		Tensile strength		Elongation, percent	Reduction in area, percent	0.2-Percent yield strength		Tensile strength		Elongation, percent	Reduction in area, percent	0.2-Percent yield strength		Tensile strength		Elongation, percent	Reduction in area, percent
				psi	N/m^2	psi	N/m^2			psi	N/m^2	psi	N/m^2			psi	N/m^2	psi	N/m^2		
Swaged W-Hf-C alloys																					
				Testing temperature, 2500° F (1644° K)						Testing temperature, 3000° F (1922° K)						Testing temperature, 3500° F (2200° K)					
A194	W-0.23Hf-0.21C	0.91	0.35	48.1×10^3	332×10^6	66.4×10^3	457×10^6	16.2	76.3	39.0×10^3	269×10^6	42.7×10^3	395×10^6	16.1	80.3	13.1×10^3	137×10^6	22.4×10^3	154×10^6	[illegible]	83.4
A156	W-0.26Hf-0.68C	2.65	42	55.5	382	57.0	392	15.5	81.7	25.0	172	46.5	320	16.[illegible]	[illegible]8.0	[illegible]	[illegible]	[illegible]	[illegible]	[illegible]	-
A218	W-0.31Hf-0.87C	2.80	51	71.0	488	78.8	543	10.8	57.4	52.7	363	57.9	400	18	[illegible]3.[illegible]	[illegible]	[illegible]	[illegible]	[illegible]	[illegible]	-
A192	W-0.44Hf-0.18C	40	30	48.4	333	56.9	392	20.0	91.3	27.3	188	38.9	268	22.0	[illegible]0.[illegible]	13.0	131	23.0	159	[illegible]	92.5
[illegible]	[illegible]	[illegible]	[illegible]	[illegible]	[illegible]	[illegible]	[illegible]	[illegible]	[illegible]	32.0	221	46.3	319	[illegible]	[illegible]	[illegible]	[illegible]	[illegible]	[illegible]	[illegible]	[illegible]
A193	W-0.48Hf-0.50C	1.03	82	35.8	247	69.0	475	13.7	91.0	47.2	325	49.5	342	7.[illegible]	91.3	29.6	197	36.6	252	[illegible]	88.0
A191	W-0.91Hf-0.94C	1.04	1.5	53.0	365	60.6	418	13.8	81.4	36.5	252	42.0	289	[illegible]7.9	79.6	[illegible]	[illegible]	[illegible]	[illegible]	[illegible]	
A190	W-1.68Hf-0.28C	17	48	[illegible]	[illegible]	[illegible]	[illegible]	[illegible]	[illegible]	45.2	312	50.0	345	[illegible]5.0	55.0	[illegible]	[illegible]	[illegible]	[illegible]	[illegible]	
A174	W-1.76Hf-0.72C	41	1.2	60.0	413	77.3	[illegible]	23.7	79.0	26.8	185	49.2	339	[illegible]9.7	85.4	[illegible]	[illegible]	[illegible]	[illegible]	[illegible]	
Recrystallized W-Hf-C alloys[a]																					
				Testing temperature, 2500° F (1644° K)						Testing temperature, 3000° F (1922° K)						Testing temperature, 3500° F (2200° K)					
A194	W-0.23Hf-0.21C	0.91	0.35	34.9×10^3	240×10^6	58.3×10^3	402×10^6	21.2	61.5	28.6×10^3	197×10^6	72.0×10^3	496×10^6	7.2	14.1	27.8×10^3	191×10^6	30.4×10^3	210×10^6	13.6	44.7
A156	W-0.26Hf-0.68C	2.65	42	29.0	200	58.8	405	16.4	97.6	35.6	245	61.7	425	24.2	97.5	27.7	191	35.1	242	[illegible]	[illegible]
A218	W-0.31Hf-0.87C	2.80	51	[illegible]	[illegible]	[illegible]	[illegible]	[illegible]	[illegible]	[illegible]	[illegible]	[illegible]	[illegible]	[illegible]	[illegible]	31.4	216	44.4	306	[illegible]	83.7
A192	W-0.44Hf-0.18C	40	30	38.[illegible]	273	67.3	477	19.0	52.7	32.0	221	60.7	418	[illegible]	[illegible]	30.2	208	33.0	227	14.6	33.0
[illegible]	[illegible]	[illegible]	[illegible]	[illegible]	[illegible]	[illegible]	[illegible]	[illegible]	[illegible]	44.8	309	73.7	507	15.9	48.6	[illegible]	[illegible]	[illegible]	[illegible]	[illegible]	[illegible]
A193	W-0.48Hf-0.50C	1.03	82	4[illegible]0	290	72.8	502	15.0	78.7	40.2	277	75.7	522	[illegible]	[illegible]	35.0	251	38.5	265	16.0	88.7
A191	W-0.91Hf-0.94C	1.04	1.5	4[illegible]2	318	73.8	508	15.4	79.0	38.5	265	51.3	354	3.6	13.1	29.1	201	33.0	228	53.7	93.5
A190	W-1.68Hf-0.28C	17	48	(b)	(b)	(b)	(b)	(b)	(b)	(b)	(b)	(b)	(b)	(b)	(b)	(b)	(b)	(b)	(b)	(b)	(b)
A174	W-1.76Hf-0.72C	41	1.2	43.4	299	67.8	467	24.8	98.3	29.7	205	50.6	349	40.7	90.2	23.9	165	32.5	224	60.0	99.2

[a]Specimens were recrystallized by annealing for 1 hr at 4400° F (2700° K).

[b]No data in recrystallized condition.

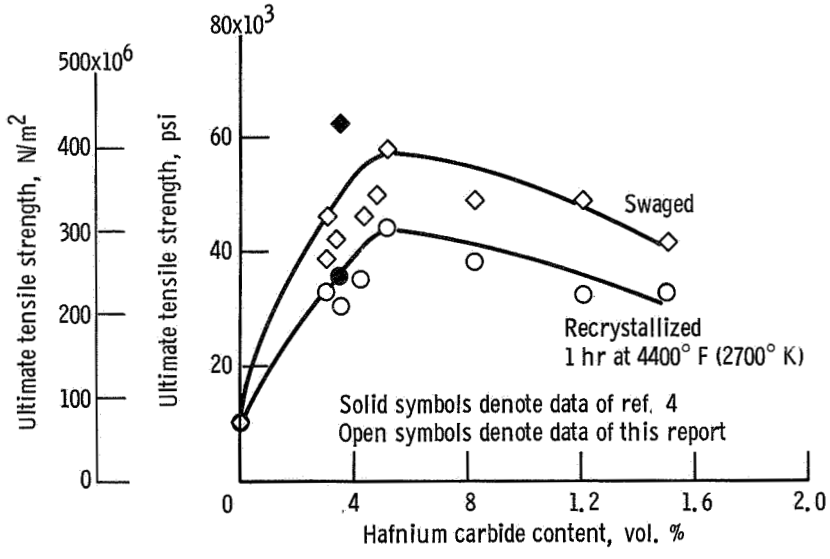

Figure 1. - Effect of hafnium carbide content on 3500° F (2200° K) ultimate tensile strength of swaged or recrystallized W-Hf-C alloys.

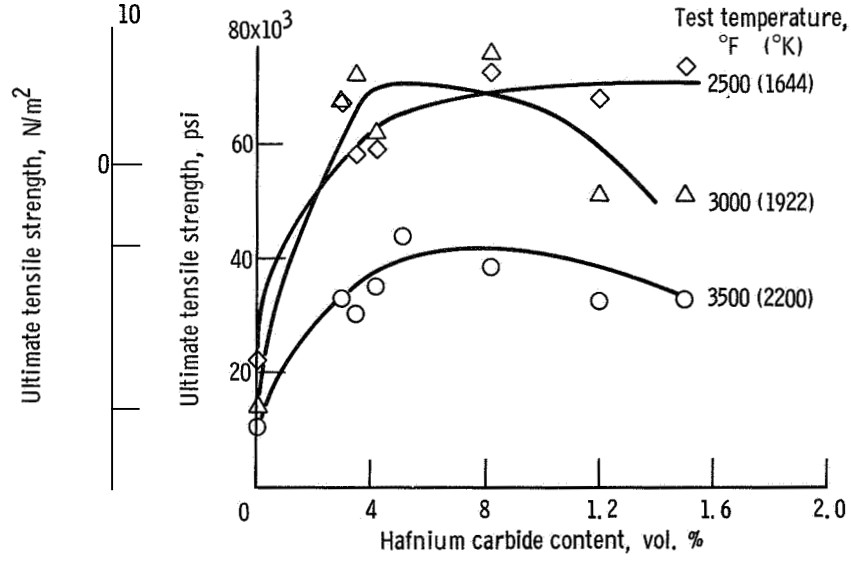

Figure 2. - Comparison of effects of hafnium carbide content on 3500° F (2200° K), 3000° F (1922° K), and 2500° F (1644° K) tensile strengths of recrystallized (1 hr at 4400° F (2700° K) W-Hf-C alloys.

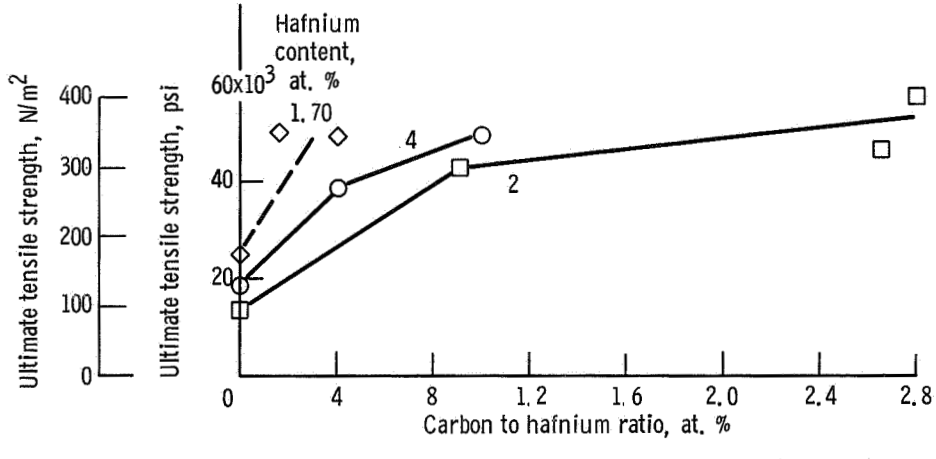

Figure 3. - Effect of carbon to hafnium ratio on 3500° F (2200° K) ultimate tensile strength of W-Hf-C alloys in swaged condition.

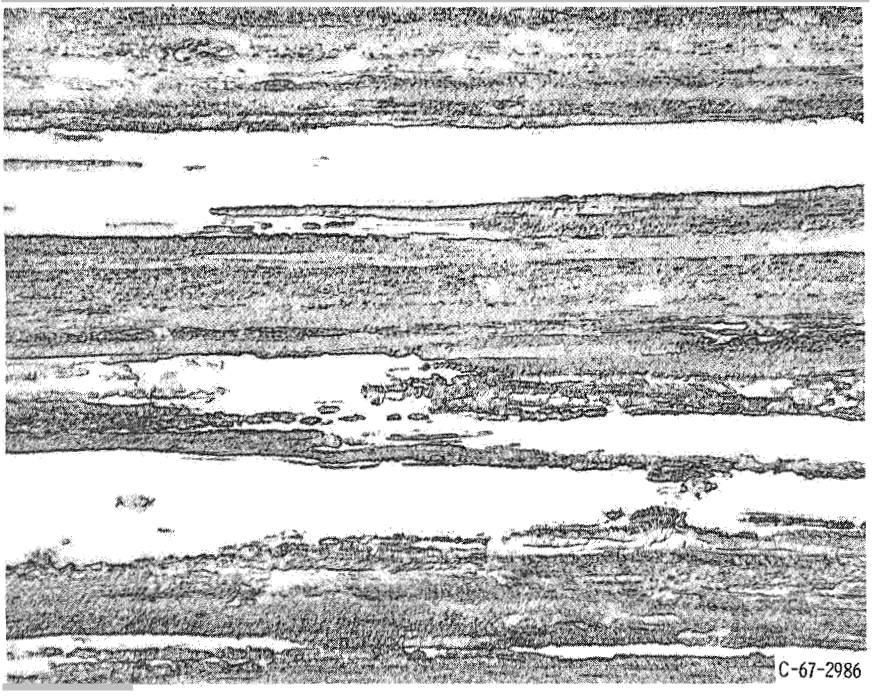

Figure 4 Optical micrograph of swaged W–Hf–C rod. Ingot, A191 composition (at. %) W–0.91Hf–0.94C X500.

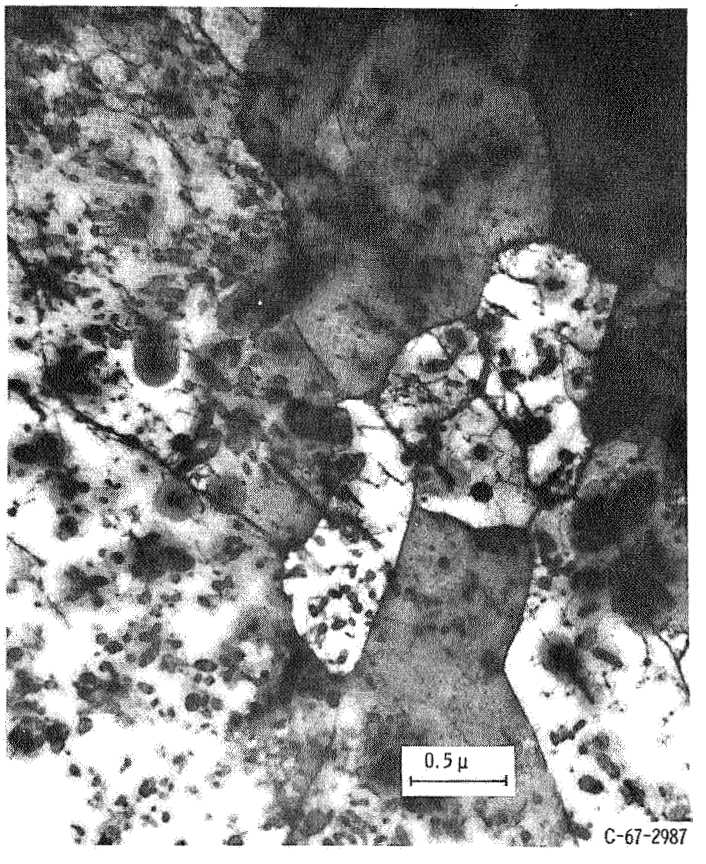

Figure 5. Electron transmission micrograph of typical structure of swaged rod. Ingot A191 composition (at. %) W–0.91Hf–0.94C. X27 500

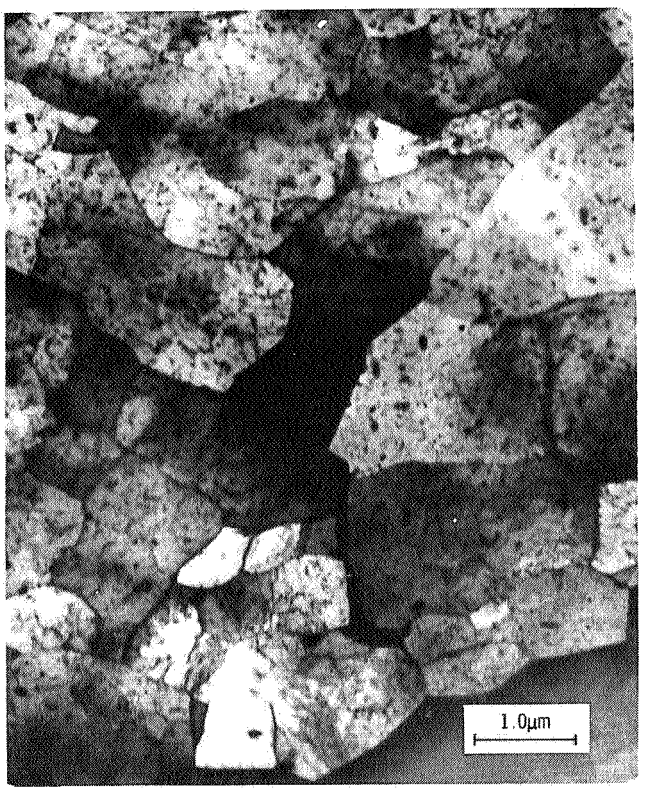

(a) Ingot A146; composition (at. %), W-0.20Hf-0.21C; average cell size, 1.0 micron X13 500.

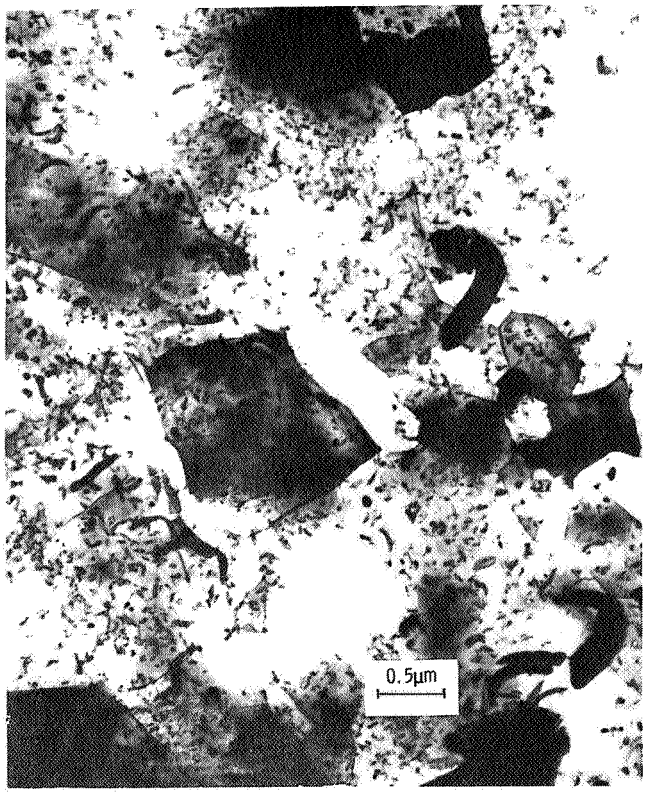

(b) Ingot A191 composition (at. %), W-0.91Hf-0.94C; average cell Size, 2.2 microns X8300.

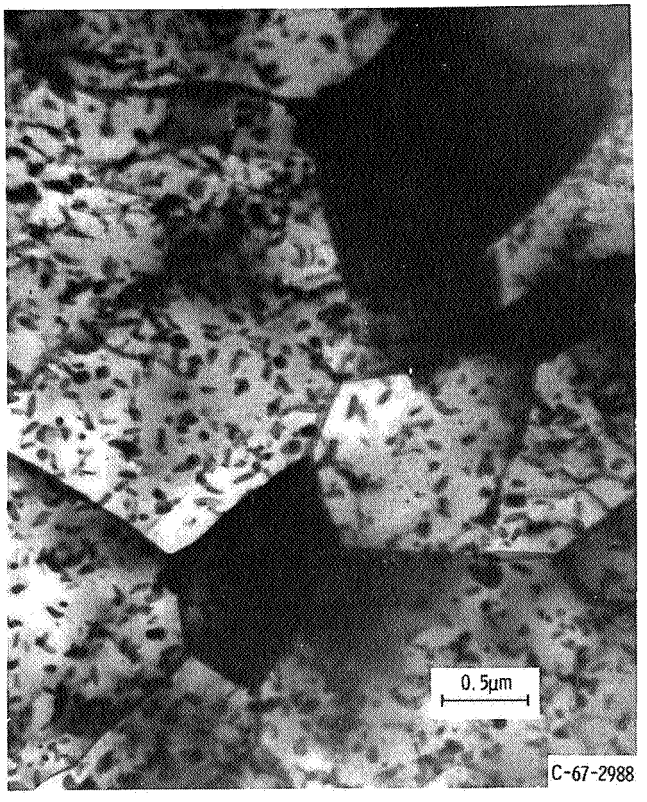

(c) Ingot A193· composition (at. %), W-0.48Hf-0.50C; average cell size, 1.6 microns. X23 300.

Figure 6. Electron transmission micrographs of typical structures of swaged tensile specimens tested at 3500° F (2200° K).

content. Although the data are limited, they suggest that carbon additions in excess of the stoichiometric composition are much less effective in promoting high-temperature strength than are lower carbon additions. This was also observed using the data of reference 5.

Structure of Swaged Alloys

The effects of particles or substructure in these W-Hf-C alloys could not be adequately observed by optical microscopy techniques. A micrograph (×500) of swaged W-0.91 Hf-0.94C (fig. 4) shows a worked structure, but no individual particles are discernible. For this reason, transmission electron microscopy was required to observe the particles and substructures which resulted from heat treatment and testing. Figure 5 is a transmission micrograph of the structure in swaged rod of the same alloy at a magnification of 27 000. The individual particles of hafnium carbide can be seen at this high magnification.

Transmission electron micrographs of typical areas representative of the structures of three alloys tensile tested to failure at 3500° F (2200° K) in the swaged condition and displaying variations in cell sizes among them are presented in figure 6. The tensile strengths of these and similar alloys were found to be linearly related to the inverse square root of their subgrain size (see fig. 7 and table III). It may be seen that the substructures of these specimens are composed of well formed cells with straight sides, and contain fine precipitate particles which are located in the boundaries and in the cell

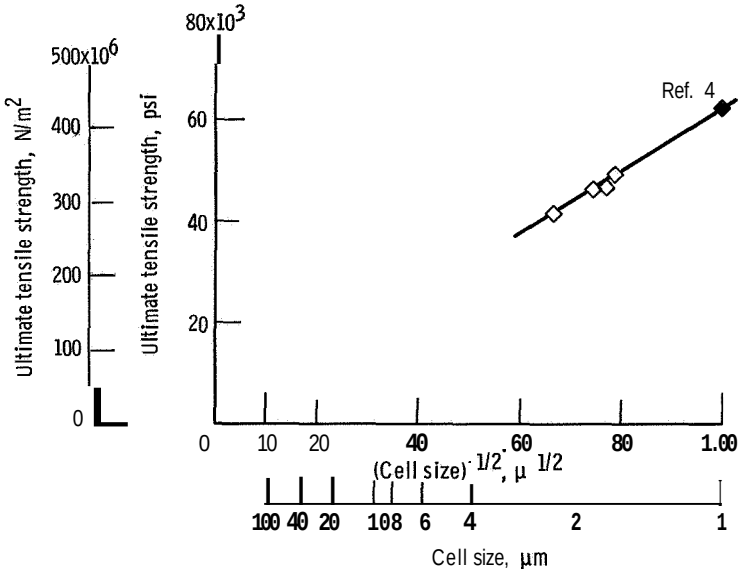

Figure 7 Effect of cell size on 3500° F (2200° K) tensile strength of swaged W-Hf-C alloys.

TABLE III. - CELL SIZES OF TENSILE

SPECIMEN TESTED TO FAILURE

AT 3500' F (2200' K)

[Specimen type, tensile.]

Ingot	Measured cell diameter, μm		
		psi	N/m^2
[a]A146	1 0	62.5×10^3	415×10^6
A156	1 68	46. 5	320
A191	2. 2	42. 0	289
A192	1 79	46. 3	319
A193	1 6	49 5	342

[a]Ref 4.

Figure 8. Electron transmission micrograph of swaged W-Hf-C specimen Ingot A191: composition tat, %), W-0.91Hf-0.094C X69 000.

interiors. The particles were identified to be hafnium carbide both by selected area electron diffraction and by Debye-Scherrer photograms of extracted particles. Selected area electron diffraction spots of specimens representative of the swaged condition (fig. 5) indicate small misorientations (approximately 5^{O}) across the subgrain boundaries. Figure 8 is an electronmicrograph of swaged material which shows a cell interior of material in the swaged condition. An example of the extremely effective pinning by particles may be seen at **A** in the figure. **A** fine particle stabilized dislocation network can be seen within the subgrain interiors.

Microstructure of Solution-Annealed and Aged Alloys

The solution and aging reaction was studied by transmission electron microscopy. Specimens were heated for $7\frac{1}{2}$ hours at 4400^{O} F (2700^{O} K), rapidly cooled in the water

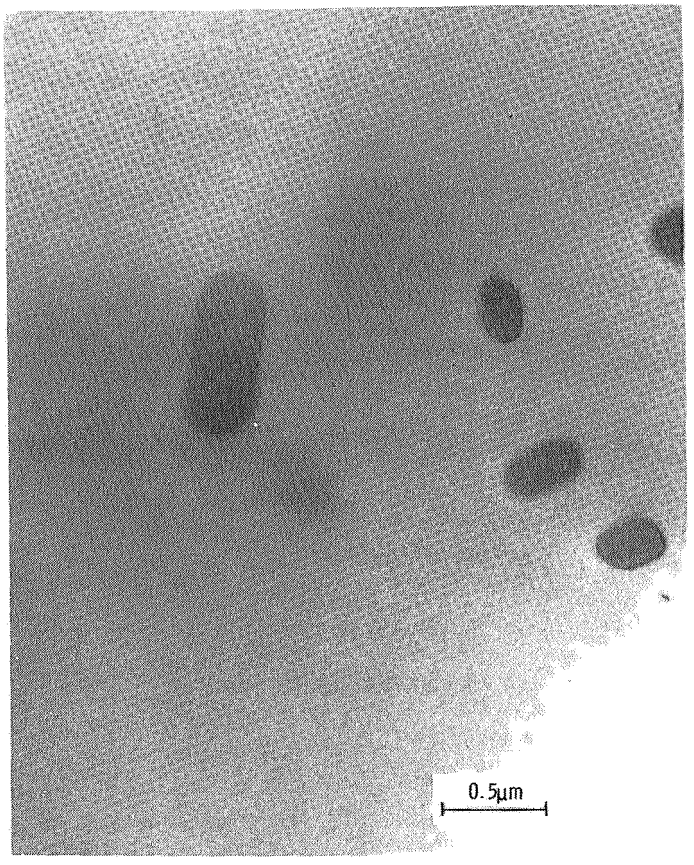

C-67-2990

Figure 9 Electron transmission micrograph of swaged specimen annealed 7 5 hours at 4400° F (2700" K) Ingot A191. composition (at. %), W-0.91Hf-0.94C. X23 000

jacketed furnace, and examined by thin film transmission. The structure contained relatively large, regularly shaped precipitates in a dislocation free matrix (fig. 9). This treatment temperature was apparently below that required for complete solutioning. However, examination of the pertinent binary phase diagrams indicated that there existed sufficient solubility at this temperature for some supersaturation of solution. After aging for 1 hour at 2000° F (1366° K), small spherical particles such as those at A in figure 10 were observed in addition to the larger regularly shaped particles at B (fig. 10) previously seen.

A second specimen of the same alloy was solution annealed for 15 minutes at 5000° F (3030° K) and quenched at greater than 1000° F (556° K) per minute by introducing helium gas to the vacuum chamber. Fine spherical precipitates were again observed (fig. 11), indicating that the cooling rate was insufficient to maintain full supersaturation.

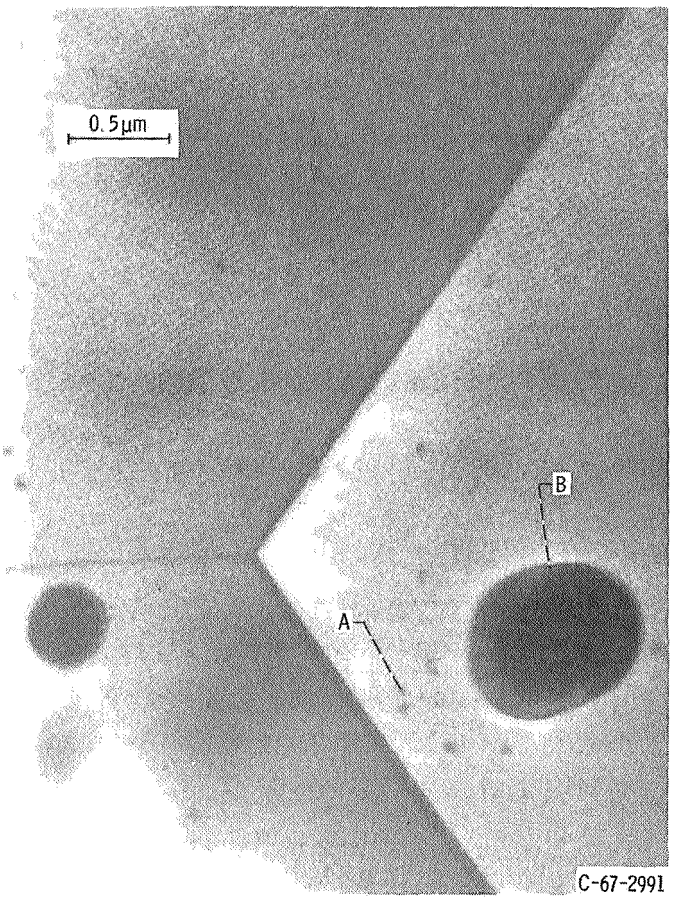

Figure 10. Electron transmission micrograph of swaged specimen annealed 75 hours at 4400° F (2700° K) and aged 10 hours at 2000° F (1366° K) Ingot A191; composition (at %), W-0.91Hf-0.94C. X23 000.

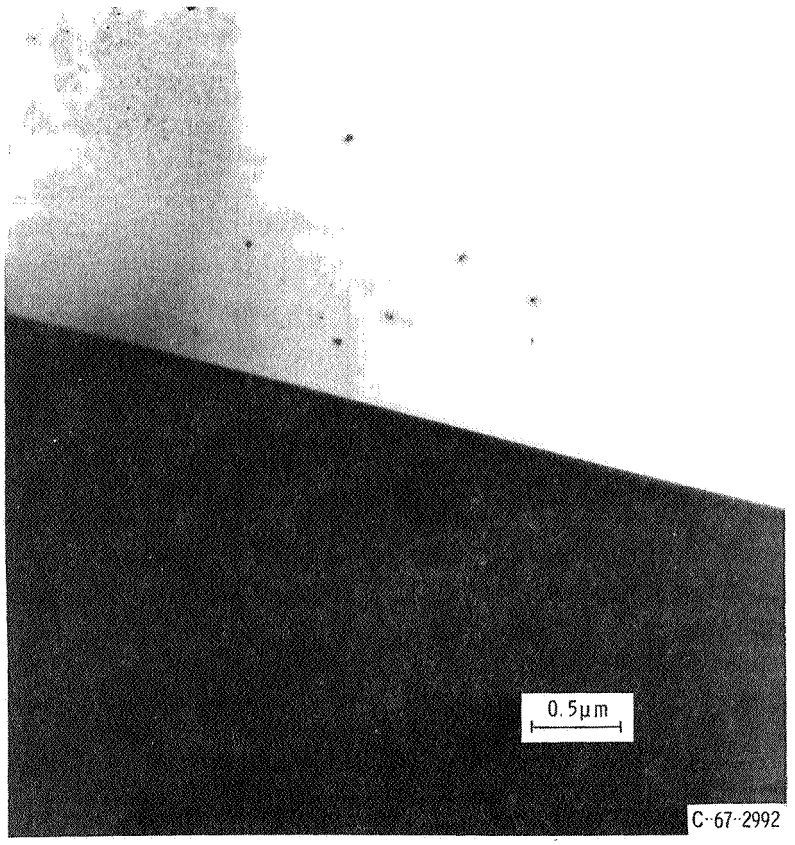

Figure 11 Electron transmission micrograph of W-Hf-C specimen. Solution annealed 1/3 hour at 5000° F (3030° K): helium quenched Ingot A191 composition (at %), W-0 91Hf-0.94C X27 500.

Effect of Heat Treatments on Tensile Properties

A summary of the 3500° F (2200° K) tensile test results derived from a solution and aging study is compiled in table IV for specimens from ingots A193 (W + 0.48Hf t 0.50C) and A191 (Wt 0.91Hf t 0.95C). This latter ingot had a carbon to hafnium ratio of 1.04 and a calculated hafnium carbide content of 1.5 volume percent. The solutioning treatment for 15 minutes at 5000° F (3030° K) was effective in increasing the 3000° F tensile strength over that attained in the swaged or recrystallized condition. But, subsequent heating at 3000° F (2255° K) decreased the strength as a result of overaging of the precipitation particles. Therefore, a different heat-treatment schedule (see table 111) was applied to ingot A193 which has a carbon to hafnium ratio of 1.03, and a calculated hafnium carbide content of 0.82 volume percent. The sharp increase in tensile strength after annealing at 4600° F (2810° K) indicates that this is the minimum solution temperature for hafnium carbide. The tensile strength was further increased by aging at 2000° to 3000° F (1366° to 1922° K) to induce precipitation of fine hafnium

TABLE IV - HIGH-TEMPERATURE TENSILE PROPERTIES OF SOLUTION ANNEALED AND AGED W-Hf-C ALLOYS

[Testing temperature, 3500° F (2200° K)]

Annealing conditions			0.2-Percent yield strength		Tensile strength		Elongation, percent	Reduction in area, percent	Post-test carbon content, ppm
Time, hr	Temperature		psi	N/m^2	psi	N/m^2			
	°F	°K							
Ingot A191; composition (at. %) W-0.91Hf-0.95C									
As-swaged			36.5×10^3	252×10^6	42.0×10^3	290×10^6	47 9	79.6	---
1	4400	2700	29.1×10^3	201×10^6	33.0×10^3	228×10^6	53.7	93.5	---
1/4	5000	3030	41.3	285	54.8	378	----	83.8	---
1/4	[a]3600	2255	36 9	254	41 5	286	----	91.5	---
1/2	[a]3600	2255	31 7	218	35.7	246	59.2	89.5	---
1	[a]3600	2255	33.5	231	37 3	257	----	----	---
Ingot A193; composition (at. %) W-0.48Hf-0.50C									
As-swaged			47 2x10:[3]	325×10^6	49.5×10^3	341×10^6	7 3	91.3	---
1	4400	2700	35.0×10^3	242×10^6	38.5×10^3	265×10^6	16 0	88,7	330
1/4	4600	2810	39.5	272	51.6	356	16,1	87 0	270
---	-----	----	50.5	348	58.3	402	14.3	82,2	233
1/4	4800	2920	43.8	302	59.2	407	----	27 4	235
1/4	5000	3030	41,5	286	55.0	379	----	21,7	170
1	[b]2000	1366	58.7	404	60.5	417	----	81.7	255
1	[b]2500	1644	50.4	348	69.0	476	----	75.0	255
1	[b]3000	1922	55.8	394	66,8	460	----	77 2	248

[a]Solution annealed 1/4 hr at 5000° F prior to indicated aging treatment,
[b]Solution annealed 1/4 hr at 4600° F prior to indicated aging treatment.

carbide particles. The highest strength was observed after aging at 2500° F (1644° K), indicating that this is close to the optimum aging temperature. The 3500° F (2200° K) tensile strength of 69 000 psi (475×10^6 N/m ^{2}) was the highest observed in this program and represents a more than sevenfold improvement over the strength of unalloyed tungsten.

A comparison of the effects of hafnium carbide content on the 3500° F (2200° K) tensile strength of recrystallized, solution-annealed, and solution-annealed and aged alloys is presented in figure 12. A large increase in strength for the solution-annealed and aged specimens relative to the strengths of the materials in the swaged (fig. 1)or recrystallized conditions may be noted.

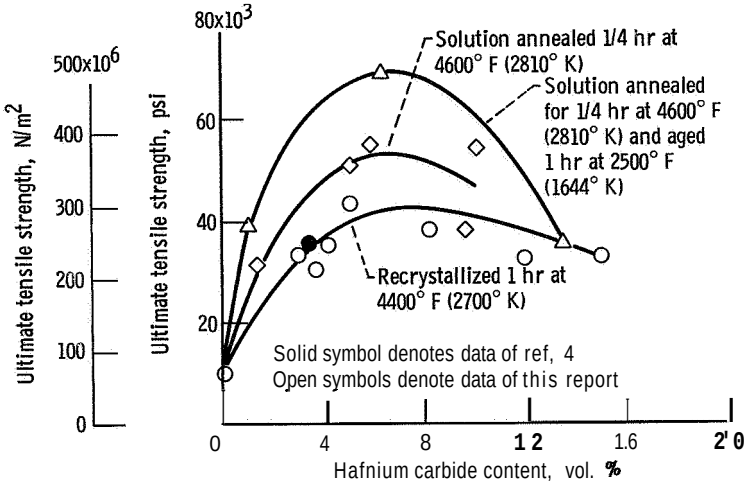

Figure 12, Effect of hafnium carbide content on 3500° F (2200° K) ultimate tensile strength for W-Hf-C alloys after various heat treatments.

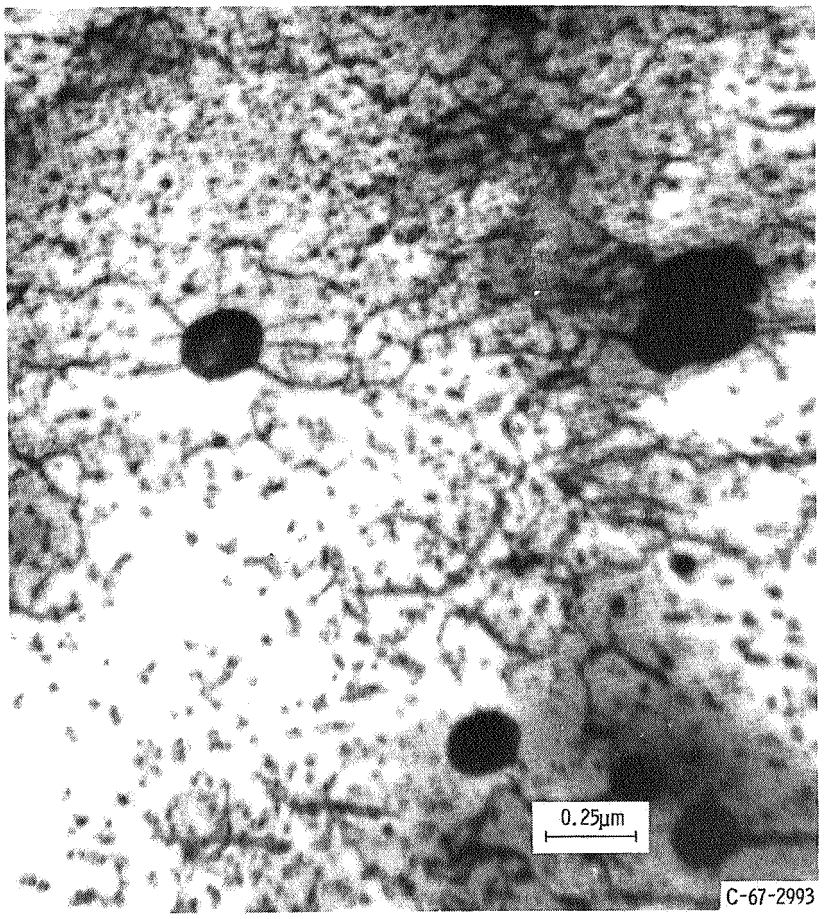

Figure 13. Electron transmission micrograph of tensile specimen tested at 3500" F (2200° K) Specimen was solution annealed for 114 hour at 4600° F (2810° K) prior to testing ingot A193; composition (at. %), W-0.48Hf-0.50C X46 600.

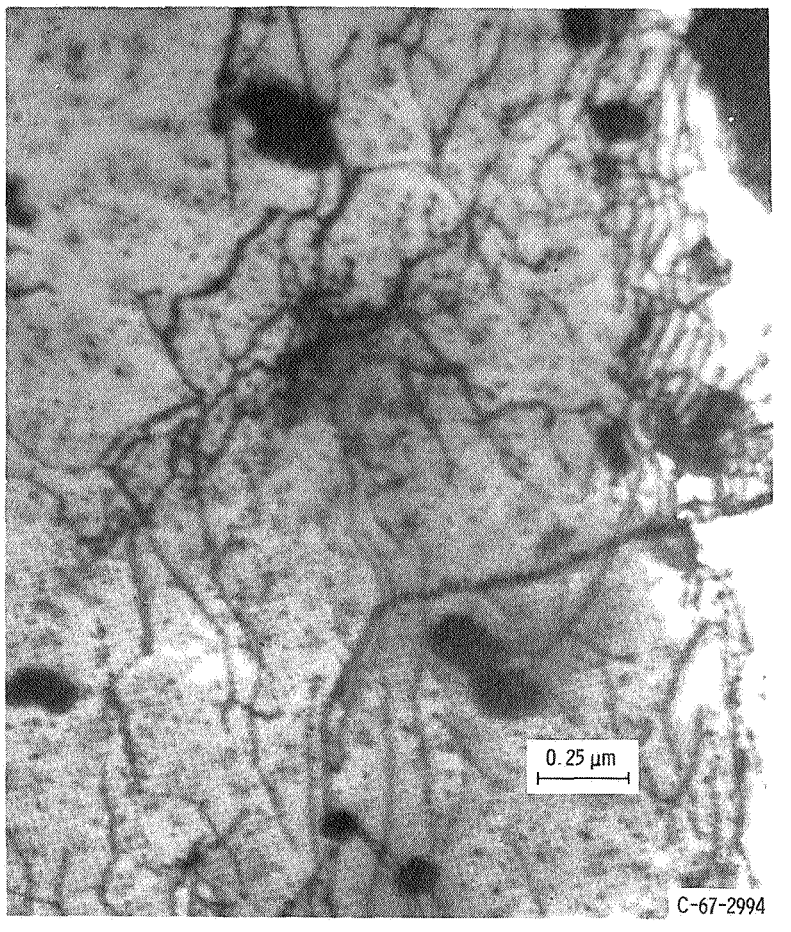

Figure 14. Electron transmission micrograph of tensile specimen tested at 3500° F (2200° K). Specimen was solution annealed for 1/4 hour at 4600° F (2810° K) and aged for 1 hour at 2500° F (1644° K) prior to testing. Ingot A190; composition (at. %), W-1.68Hf-0.28C. X46 600.

Some transmission micrographs of solution-annealed, and solution-annealed and aged specimens tensile tested to failure are presented in figures 13 and 14. In these specimens no regular cell structure is observed, but they are characterized by a large amount of small precipitate particles evenly distributed throughout the matrix. A fine network of dislocations may be seen to have formed (see A, fig. 14) between the larger particles which act as anchoring points.

High-Temperature Creep Testing

Results of step-load creep tests on annealed W-Hf-C alloys and of creep-rupture tests on swaged alloys at 3500° F (2200° K) are summarized in table V. A comparison of typical minimum creep rates as a function of initial stress, obtained from step-load creep tests for annealed W, W-Hf (ref. 4), and W-Hf-C alloys, is presented in figure 15. The precipitation-hardened material is significantly more resistant to creep than the

TABLE V EFFECT OF COMPOSITION AND HEAT TREATMENT ON 3500° F (2200° K) CREEP PROPERTIES OF W-Hf-C ALLOYS

(a) Step-load creep of recrystallized or solution-annealed alloys

Ingot	Composition, at. %	Stress, psi	Stress, N/m^2	Minimum creep rate ϵ, sec^{-1}
A190	W-1 68Hf-0. 28C	8 370	57.7×10^6	5.8×10^{-8}
		9 85(	67. 9	5.4×10^{-7}
		11 81(	81,4	$1\ 5\times10^{-6}$
		14 29(	98. 5	4.4×10^{-6}
		16 73(	115	$1\ 0\times10^{-5}$
		19 20(	132	2.2×10^{-5}
A193	W-0, 48Hf-0. 72C	8 89C	$61,3\times10^6$	2.1×10^{-8}
		10 63C	73. 3	$7\ 4\times10^{-8}$
		12 75C	87. 9	$1\ 7\times10^{-6}$
		14 69C	101	8.7×10^{-6}
		16 61C	115	4.4×10^{-5}
A174	W-1 76Hf-0. 72C	8 40C	57.9×10^6	9.3×10^{-7}
		10 85C	74.8×10^6	$7\ 7\times10^{-5}$
A191	W-0. 91Hf-0. 94C	9 76C	67.3×10^6	9.2×10^{-8}
		12 60C	$86,9\times10^6$	2.3×10^{-7}
		16 650	115×10^6	3.4×10^{-6}
A156	W-0. 26Hf-0. 66C	10 000	$68\ 9\times10^6$	$1\ 3\times10^{-7}$
		12 670	$87\ 4\times10^6$	4.0×10^{-6}
		14 710	101×10^6	$2,8\times10^{-5}$
A193	[a]W-0, 48Hf-0. 50(	8 770	60.5×10^6	5.1×10^{-8}
		10 800	74.5	2.0×10^{-7}
		15 500	107	6.7×10^{-7}
		18 800	130	$1\ 6\times10^{-6}$
		24 500	169	5.9×10^{-4}
A174	[a]W-1 76Hf-0. 72(	9 300	64.1×10^6	$1\ 1\times10^{-7}$
		11 200	77 2	2.7×10^{-7}
		13 320	91 8	8.3×10^{-7}
		15 820	109	3.4×10^{-6}
A192	W-0, 44Hf-0, 18C	7 000	48.3×10^6	$1\ 1\times10^{-7}$
		8 270	57 0	$7\ 6\times10^{-7}$
		9 960	68. 7	3.3×10^{-6}
		11 880	81 9	$1\ 2\times10^{-5}$
		14 000	96. 5	5.3×10^{-5}
A194	W-0, 23Hf-0, 21C	9 060	62.5×10^6	$1\ 7\times10^{-6}$
		10 600	73.1×10^6	$3\ 7\times10^{-6}$
		12 810	88.3×10^6	$1\ 5\times10^{-4}$
4193	[b]W-0. 48Hf-0. 50(	16 600	114×10^6	$1\ 51\times10^{-7}$
		17 830	123	3.31×10^{-7}
		19 100	132	3.38×10^{-7}
		13 600	163	$1\ 29\times10^{-6}$
		16 200	181	4.36×10^{-5}
		27 000	186	$1\ 27\times10^{-4}$
		27 800	192	$3\ 86\times10^{-4}$

(b) Step-load minimum creep rate of recrystallized or solution-annealed alloys

Ingot	Composition, at. %	Stress for minimum creep rate of 10^{-6} sec^{-1}, psi	Stress for minimum creep rate of 10^{-6} sec^{-1}, N/m^2
A190	W- 1.68Hf-0.28 C	11 200	77 $\times10$
A193	W-0.48 Hf-0. 72 C	12 200	84
A174	W-1 76 Hf-0. 72 C	8 400	57 9
A191	W-0.91 Hf-0. 94 C	14 700	101
A156	W-0.26 Hf-0.66 C	11 400	78. 5
A193	[a]W-0. 48 Hf-0.50 (	17 000	117
A174	[a]W-1 76 Hf-0.72 (	13 700	94 4
A192	W-0.44 Hf-0.18 C	8 500	58.5
A194	W-0.23 Hf-0.21 C	9 000	62
A193	[b]W-0. 48 Hf-0. 50 (	23 000	159

(c) Creep rupture of as-swaged alloys

Ingot	Composition, at. %	Stress, N/m^2	Steady creep, sec^{-1}	Rupture time,
A190	W- 1. 68 Hf-0. 28 C	17 900	123 $\times10^{(}$	4.4×10^{-6}	12. 6
A193	W-0. 48 Hf-0. 72 C	9 920	69. 4	4.7×10^{-8}	262
A174	W- 1. 76 Hf-0. 72 C	8 600	59. 3	4.5×10^{-7}	167 5
A191	W-0. 91 Hf-0. 94 C	14 470	99. 5	3.5×10^{-7}	91. 0
A156	W-C. 26 Hf-0. 66 C	6 860	47, 3	5.3×10^{-8}	127 5
A192	W-0. 44 Hf-0. 18 C	10 780	74. 2	2.0×10^{-6}	83. 6
A194	W-0. 23 Hf-0. 21 C	15 000	104	6.3×10^{-7}	22. 8

'Solution annealed 1/4 hr at 5000° F (3030° K); helium quenched.
'Solution annealed 1/4 hr at 4650° F (2840° K); helium quenched; aged 1 hr at 2500° F (1644° K)

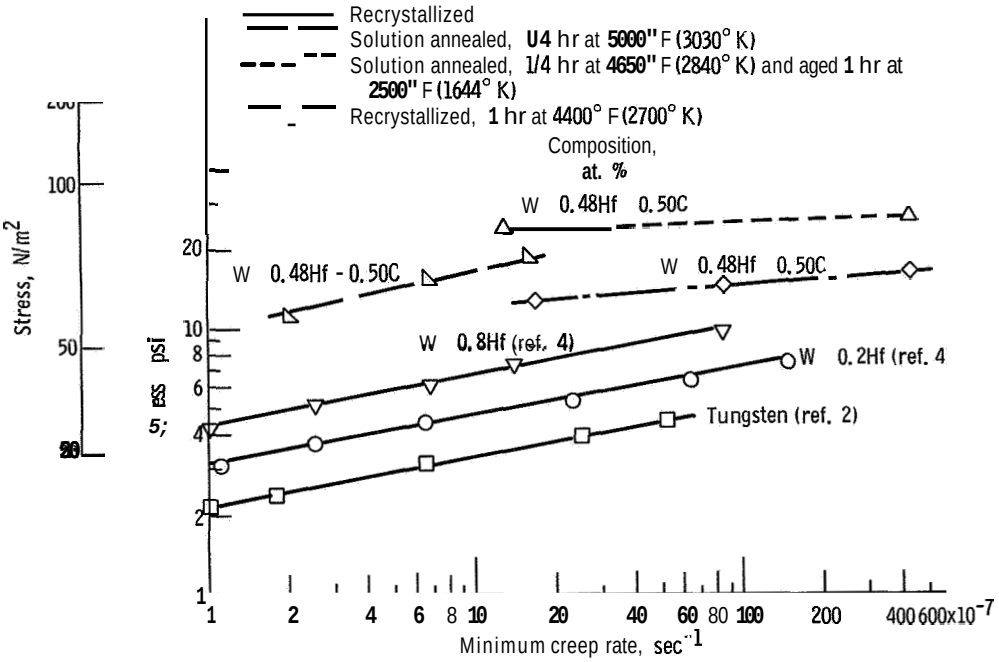

Figure 15. Stress dependence of minimum creep rate from step-load creep tests at 3500" F (2200° K) for W, W-Hf, and W-Hf-C alloys.

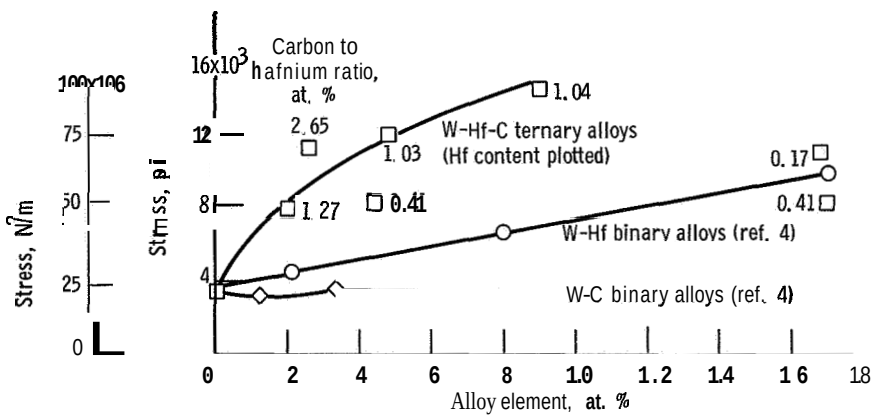

Figure 16. Effect of carbon or hafnium content on stress for minimum creep rate, at 3500° F (2200° K), of 10^{-6} sec^{-1} from step-load creep tests of recrystallized alloys,

solid solution strengthened alloys, but shows a greater stress dependence of minimum creep rate. For example, where the stress dependence of creep rate is represented by a power law ($\dot{\epsilon} \alpha \sigma^n$), the stress exponents for the alloys listed in table V and shown in figure 15 vary between 10 and 13, as compared to about 5 for the arc-melted W and the W-Hf binaries. The stress exponent of the solution annealed W-Hf-C specimen (fig. 16) is also approximately 5.

The effect of carbon or hafnium content on the stress for a creep rate of 10^{-6} second $^{-1}$, obtained from 3500° F (2200° K) step-load creep tests of W binary alloys by Raffo and Klopp (ref. 4), is shown in figure 16. The stresses obtained with the

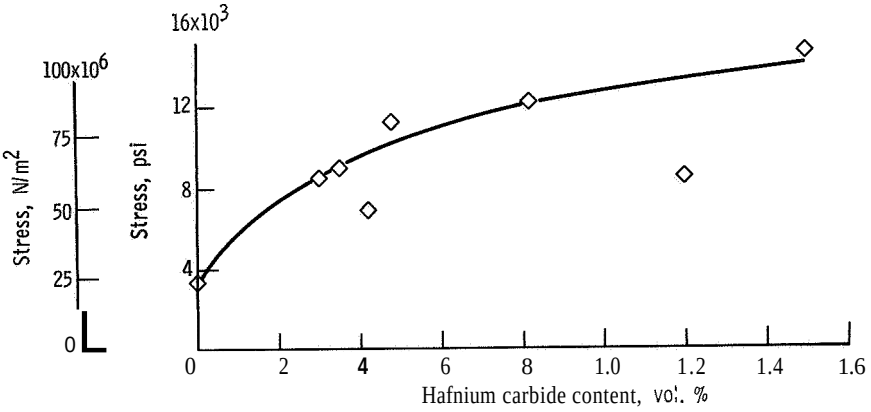

Figure 17 Effect of hafnium carbide content on stress for a minimum creep rate of 10^{-6} sec $^{-1}$ for W-Hf-C alloys tested in the recrystallized condition by steploaded creep at 3500° F (2200° K).

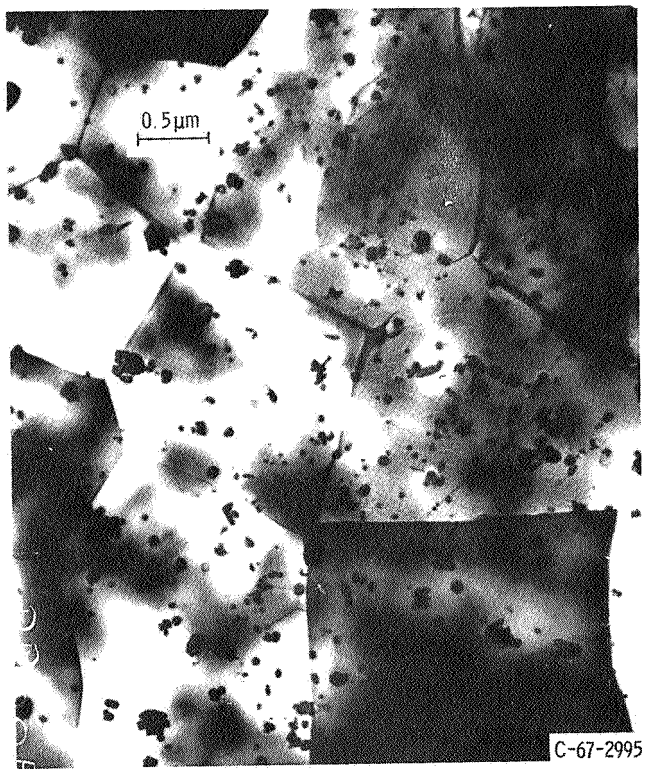

Figure 18. Electron transmission micrograph of typical structure of swaged creep rupture specimen tested to failure at 3500° F (2200° K). Ingot A191 composition (at. %), W-0.91Hf-0.94C; average cell size, 3.0 microns. X16 500.

W-Hf-C alloys for the same creep rate are plotted against hafnium content and the carbon to hafnium ratios are indicated. The alloys whose ratios are appreciably less than 1 have strengths which approximate those of the W-Hf binary alloys while those whose ratios approximate 1 lie on a line well above those of the binaries.

Figure 17 shows the effect of increasing hafnium carbide content on the stress for a minimum creep rate of 10^{-6} second^{-1}, for the alloys tested at 3500° F (2200° K) in stepload creep. Strength continued to increase with hafnium carbide content up to a value of 14 700 psi (101×10^6 N/m^2) at a precipitate content of 1.5 volume percent. This compares with a value of approximately 35 000 psi for unalloyed tungsten.

Figure 18 is transmission micrograph of a swaged creep-rupture specimen of W-0.91Hf-0.94C tested to failure in approximately 91 hours at 3500° F (2200° K). It may be observed that the particles have coarsened, relative to those observed in swaged but untested material shown in figure 5, and that the cell interiors are relatively free of dislocation structure.

The elevated temperature tensile ductility data is summarized in tables II and III for the swaged and recrystallized alloys, respectively. The effect of increasing hafnium carbide content in the recrystallized alloys is to increase the reduction-in-area, which is essentially independent of test temperature in the 2500° to 3500° F (1644° to 2200° K) range. The effect of hafnium carbide content on total elongation at failure was similar to that observed for reduction-in-area; however, test temperature effects were more pronounced and the specimens tested at higher temperatures had higher elongations. The ductility of specimens tested in the swaged condition was relatively insensitive to test temperatures in the 3000° to 4000° F range. Minima in both reduction in area and elongation occur at 0.5 to 0.8 volume percent hafnium carbide.

Bend ductile-brittle (4T) transition temperatures of 40-mil sheet from ingot A191 were 350° F (450° K) for material rolled to approximately a 90-percent reduction area from the extruded condition and 400° F (478° K) after a 1-hour anneal at either 3600° or 4400° F (2255° or 2700° K). This compares to about 600° F (589° K) for unalloyed tungsten after a similar high-temperature anneal.

Recrystallization Behavior

Figure 19 shows the effect of increasing the hafnium carbide content on the 1-hour isochronal temperatures for 100 percent recrystallization of the various composition alloys. These data are for 3/8-inch-diameter (0.9525-cm-diam) rod worked approximately 83 percent. Complete recrystallization for alloys with approximately 0.5 volume percent hafnium carbide, or greater, requires annealing at temperatures of 4200° to 4300° F (2589° to 2640° K), while those with smaller dispersed particle contents (e.g., 0.3 to 0.4 volume percent HfC) have recrystallization temperatures in the

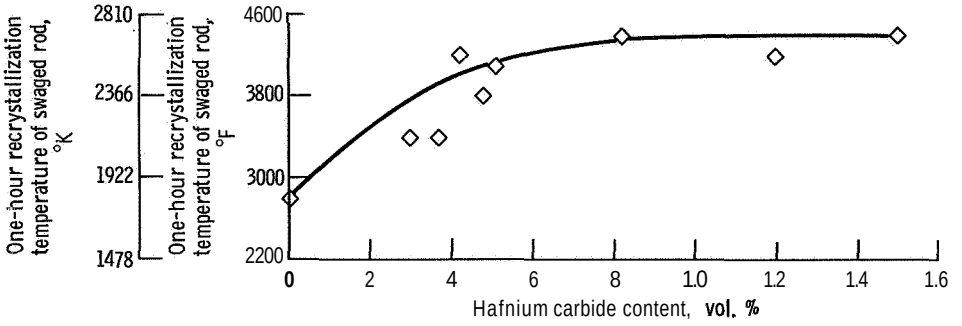

Figure 19. Effect of hafnium carbide content on 1-hour isochronal recrystallization temperature of W-Hf-C alloys,

range 3300° to 3400° F (2089° to 2144° K). These values may be compared to 2800° F (1811° K) for the complete recrystallization of arc-melted unalloyed tungsten worked a similar amount.

DISCUSSION OF RESULTS

The formation and stabilization of the dislocation substructure and its interaction with the precipitate particles is of paramount importance in the development of high-strength, high-temperature alloys. To aid in understanding the strength-substructural relations of these W-Hf-C alloys, the deformation structure of pure tungsten, the effect that fine precipitates have on this structure at high temperatures, and the factors which control precipitate morphology are considered.

Keh and Weissmann (ref. 10) have reviewed the deformation-induced structural changes which occur in unalloyed tungsten. The structure of warm-worked tungsten consisted of cells 0.5 to 2 microns (5×10^{-7} to 2×10^{-6} m) in diameter with interiors fairly clear of dislocations. It was concluded that there were few if any barriers within the cells and that the interbarrier distance equals the cell diameter.

Dispersed phase strengthening theory considers that particles act as obstacles to dislocation motion and relates the strength increases to either a dependence on inter-particle spacing or to volume fraction of particles (see Fine, ref. 11, for example). Slip proceeds by the moving dislocation passing the particle by either leaving the slip plane (climb or cross slip), or passing through the particle by shearing it, or by bowing out between the particles. This last should result in dislocation loops being left about the particle.

Recently, on the basis of direct viewing of particle-dislocation interactions in the electron microscope, it was suggested that at high temperatures fine particles are ineffective obstacles to moving dislocations in body-centered-cubic metals as cross slip could effectively prevent dislocation entrapment (refs. 12 and 13). It was suggested

that the observed particle induced strengthening arises from the generation of a finer cell size due to particle enhanced dislocation generation. The intracell dislocation network caused by the intersection of moving dislocations would serve as preferred nucleation sites for the precipitates; thus, further stabilizing the cells and aiding in the prohibition of long-range dislocation motion and easy cell growth. To understand the role that particles play in the W-Hf-C alloys it is worthwhile to consider the factors which affect precipitate size and spacing in the body-centered-cubic metals. These factors are the aging temperature, the degree of supersaturation, and the composition of the alloy (ref. 14). At high aging temperatures (low solute supersaturation), the grain and cell boundaries are preferred precipitation sites; at lower aging temperatures (higher solute supersaturation), fine particle precipitation in the matrix is more likely (ref. **14).** For example, in the iron-carbon and iron-nitrogen systems, if precipitation were restricted to dislocations present before aging, an uneven dispersion of coarse particles was obtained and the interparticle spacing was large. Compositional effects were shown by the addition of columbium to the carbon steels. Controlling the carbon and columbium composition governed the size and distribution of particles. When the solute concentrations were high, precipitation occurred at a high temperature and the particles were relatively coarser.

Tensile Behavior

Whether particles act directly as the primary obstacles or indirectly to control the deformation substructure, their size and distribution will ultimately control the strength properties. Therefore, it is necessary to consider the tensile results in terms of precipitate contents and substructural interactions. In the RESULTS section, the tensile strength was shown to depend on the hafnium carbide content (figs. **1, 2,** and 12), cell diameter (fig. 7), and carbon to hafnium ratio (fig. **3).** Also, hafnium carbide in amounts greater than about 0.5 volume percent was shown to cause a decrease in this property. In the swaged W-Hf-C alloys it may be that, at compositions of carbon or hafnium may yield precipitates in amounts greater than about 0.5 volume percent (see fig. 1), the particle spacing increases due to particle coarsening and results in the increased cell diameters and decreased tensile strengths observed. Similarly, the carbon to hafnium ratio can influence the tensile strength (fig. **3).** In alloys containing an excess of carbon, tungsten carbide particles may precipitate and serve as nucleation sites for the precipitation of hafnium carbide, thus increasing particle size and spacing.

Since tensile strength could be related to the cell sizes of the swaged and tested rod, the cell walls are the principal barriers to dislocation motion and the role of particles in this heavily worked material is to refine the cell size and then to stabilize

the cells after formation as suggested in references 12 and 13. Examination of the structures of the as-swaged (fig. 5) and swaged and tested alloys (fig. 6) showed that the former contained some large precipitates on the order of 0.1 to 0.2 micron in size and many small precipitates about 0.02 micron (2×10^{-8} m) (200 Å) in size. If the precipitates prevent passage of moving dislocations, a dislocation loop about the particles and evidence of pileups is expected. These were not observed nor were sheared particles observed. However, the bowed out and severely jogged dislocation segments between some particles (figs. 5 and 6) indicate that precipitate pinning of dislocations has occurred. This pinning may have occurred by capture of mobile dislocations or by precipitation on the already relatively immobile dislocation network formed within the cells during deformation processing. For example, the arc-melted alloys of this study were extruded at temperatures just under those used for complete precipitate dissolution, and they were swaged at temperatures slightly higher than the best aging temperature. Thus, stress-induced precipitation and consequent stabilization of the fine dislocation network formed during warm working could occur.

Figure 2 shows that there was no decline in tensile strength of the recrystallized material with increasing hafnium carbide content for the material tested at 2500° F (1644° K) and that the material tested at 3000° F (1922° K) was stronger than that tested at 2500° F (1644° K). This latter type behavior is often observed at low temperatures in body-centered-cubic metals and usually is indicated by an aging peak in the flow stress-temperature curve and by serrations in the tensile stress-strain curves. These effects at low temperatures are due to strain aging of interstitial elements. However, in the W-Hf-C alloys, which were tested at relatively higher temperatures, similar effects were observed which may be due to precipitation of hafnium carbide during testing. Such behavior was previously observed by Chang in Cb-1Zr alloys (ref. 15). For example, evidence for such stress-induced precipitation may be seen in figure 20, which shows a stress-elongation curve for a recrystallized specimen tested at 2500° F (1644° K). Serrations similar to those shown in this figure were observed on the load-elongation curves of both swaged and recrystallized specimen of most alloys. Such serrations in the stress-strain curve at high temperature probably can arise from diffusion of substitutional atoms associated with precipitation during straining (ref. 16).

A different situation existed when the transmission micrographs of the solution-annealed and the solution annealed and aged tensile specimens (figs. 13 and 14) were considered. In figures 13 and 15, the large particles acted as anchoring points, and greater dislocation densities between particles were observed. No well developed substructure with cells was observed. Rather, a copious distribution of fine particles may have exerted a strong obstacle back stress to dislocation motion. This condition was reflected in the high strengths observed in this material at 3500° F (2200° K).

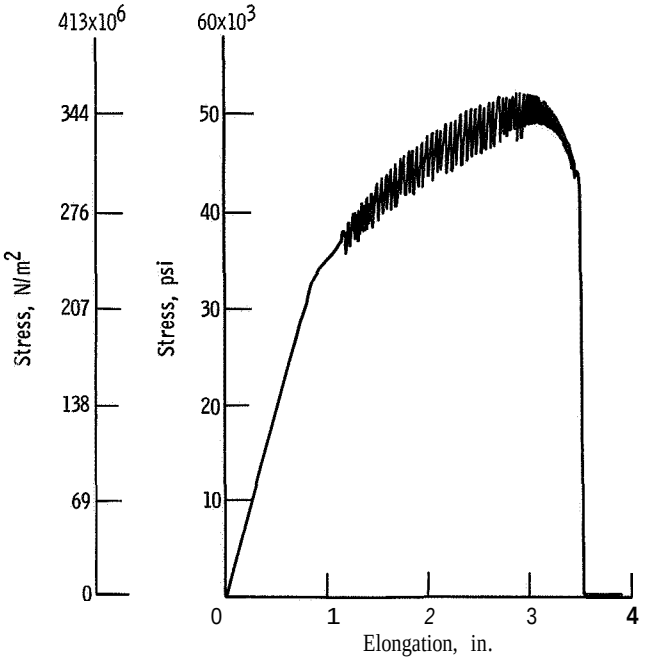

Figure 20. Stress elongation curve for recrystallized (1 hr, 4000° F (2700°K)) W-Hf-C alloy tested at 2500° F (1644° K).

Many examples of the strong pinning effects exerted by particles on dislocations may be seen in both figures.

To summarize, in the swaged and recrystallized materials, the particle size and spacing are less than optimum and many of the particle effects were realized through their influence on the resulting cell sizes that were observed to be of importance in the swaged material. In the case of the solution-annealed and aged materials, a much more ideal particle size and distribution result in effective blocking of dislocations.

Creep Behavior

Results from stepload creep tests at 3500° F (2200° K) clearly established the effectiveness of hafnium carbide particle strengthening of tungsten over that of solid solution strengthening. However, it was seen that when the stress dependence of creep rate was represented by a power law ($\dot{\epsilon} \alpha \sigma^n$) the dispersed phase material had exponents of the order of **10** to **13** compared to about n = 5 for the single phase W and W-Hf alloys. Wilcox and Clauer (ref. **17)** observed exponents of about 7 for nickel-thoria alloys with a temperature compensated creep rate as a function of log stress. This apparently high value, relative to that expected ($n \sim 4.5$) by the Ansell and Weertman theory for climb controlled dislocation motion during creep (ref. 18), was explained on the basis of the stress dependence associated with the internal stress due to the precreep substructure. Similarly, in the W-Hf-C alloys, the precipitate-stabilized fine dislocation

structure observed within the cell interiors would tend to increase greatly the internal stresses, thus resulting in the high stress dependence observed.

Hirschorn and Ansell (ref. 19) point out that mathematically there is good agreement between yield strength and either (volume percent)$^{1/3}$ or (volume percent)$^{1/2}$. However, they concluded that a three-dimensional description more accurately represents the actual distribution of dispersed phase particles. In this study the effect of increasing hafnium carbide content was analytically related to the difference between creep strengths (10^{-6} second^{-1}) of the alloyed and pure tungsten. A least squares analysis of a logarithmic plot of creep stress for the alloy less the stress for pure arc-melted tungsten against volume percent has a slope of 0.39, and it was felt that a plot of creep stress difference against (volume percent of hafnium carbide)$^{1/3}$ was a valid expression of the strength improvement due to the dispersed phase.

Recrystallization Behavior

The cell or subgrain is considered to be the recrystallization nucleus and recrystallization may occur by either cell boundary movement (ref. 20) or subgrain coalescence (ref. 21). Both mechanisms require dislocation motion, primarily within the cell interiors. Beneficial particle effects in inhibiting recrystallization could arise both from the pinning of the dislocation networks within the cells and from the prevention of cell or grain boundary motion. In the W-Hf-C alloys, the fine dislocation network established within the cellsduring warm working, could accomplish the former while the effect of the preexisting precipitate in initially preventing formation of the cells with relatively mobile boundaries could accomplish the latter. In the alloys of this study it is not clear from which effect the dependence of recrystallization temperature on hafnium carbide content arises.

CONCLUDING REMARKS

The W-Hf-C alloys have been shown to be heat treatable and capable of achieving exceptionally high tensile strengths at 3500° F (2200° K). These strengths are predicated on precipitation of small particles of hafnium carbide with small interparticle spacings. These microstructures are sensitive to alloy composition, amount of precipitate, and solution and aging temperatures. The presence of serrations in the stress-strain curves, aging peaks in the strength-test temperature plots, and the nature of the dependence of tensile strength on test temperature and hafnium carbide content suggests that the kinetics of particle precipitation and coarsening can be rapid at 3500° F (2200° K) and applications requiring exceptionally high strengths for long times at this

temperature must be examined critically. However, the inverse dependence of the tensile and probably creep strength on the cell size of the swaged material, coupled with the precipitate stabilization of the cold-worked structure to a recrystallization temperature of 4400° F (2700° K) suggests that long time intermediate temperature (e. g. , 2500° F, 1644° K) applications are practical in environments which do not cause carbon depletion in the alloy.

In the heat-treated alloys it is difficult to determine the specific nature of the particle-dislocation interactions, but the absence of dislocation cells or networks leads to the conclusion that the particles were directly responsible in controlling the tensile strength. In the case of the swaged alloys with the well developed substructures, a correlation between tensile strength and cell size was obtained. It would be worthwhile to ascertain the role that the particles or total precipitate content played in establishing the cell size, in addition to their obvious effect of stabilizing the substructure once it is formed.

CONCLUSIONS

The following conclusions relative to the effects of composition, heat treatments, and substructure on the elevated temperature mechanical properties of arc-melted W-Hf-C alloys were made:

1. The W-Hf-C alloys, previously shown to have high strength, have been further characterized and shown to be heat treatable. The strongest alloys exhibited approximately a sevenfold strength improvement over unalloyed tungsten at 3500° F (2200° K). The strength of these alloys is strongly dependent on solution and aging temperatures.

2. The 3500° F (2200° K) tensile strength of W-Hf-C alloys increases with increasing hafnium carbide content reaching a maximum at approximately 0.5 volume percent.

3. The 3500° F (2200° K) tensile strength of swaged rod is inversely proportional to the square root of the cell size of the tested material measured transverse to the tensile direction.

4. The minimum solution temperature was determined by 3500° F (2200° K) tensile testing to be approximately 4600° F (2810° K). The optimum aging temperature was similarly determined to be 2500° F (1644° K). The strengths of these specimens were related to precipitate-substructure morphology. The 3500° F (2200° K) tensile strength of a specimen in the optimum solution and aged condition was 69 000 psi (475×10^6 N/m^2).

5. The 3500° F (2200° K) creep strength, obtained from stepload creep tests, increased with increasing hafnium-carbide content, and was highest in alloys whose compositions were close to being equiatomic in carbon and hafnium. A solution-annealed and aged specimen had a 3500° F creep strength of 23 000 psi (159×10^6 N/m^2) for a minimum creep rate of 10^{-6} second^{-1}.

6. Swaged rod of alloys with hafnium carbide contents of 0.8 volume percent, or greater, have 1-hour recrystallization temperatures in excess of 4200° F (2589° K).

7. For high-strength applications at 3500° F (2200° K), compositions composed of equiatomic amounts of carbon and hafnium, approximately 0.3 to 0.4 percent, are recommended.

Lewis Research Center,
National Aeronautics and Space Administration,
Cleveland, Ohio, August 17, 1967,
129-03-02-02-22.

REFERENCES

1. Foyle, Fred A. : Arc-Melted Tungsten and Tungsten Alloys. High Temperature Materials. Vol. 18, Part 2 of Metallurgical Society Conferences. G. M. Ault, W. F. Barclay and H. P. Munger, eds., Interscience Publishers, 1963, pp. 109-124.

2. Klopp, William D.; and Raffo, Peter L. : Effects of Purity and Structure on Recrystallization, Grain Growth, Ductility, Tensile, and Creep Properties of Arc-Melted Tungsten. NASA TN D-2503, 1964.

3. Raffo, Peter L.; Klopp, William D. ; and Witzke, Walter R. : Mechanical Properties of Arc-Melted and Electron-Beam-Melted Tungsten-Base Alloys. NASA TN D-2561, 1865.

4. Raffo, Peter L.; and Klopp, William D. : Mechanical Properties of Solid-Solution and Carbide-Strengthened Arc-Melted Tungsten Alloys. NASA TN D-3248, 1966.

5. Friedman, S. ; and Dickinson, C. D. : Powder Metallurgy Tungsten Alloys Based on Carbide Dispersions. Rep. No. TR 65-351-3, General Telephone and Electronics, 1965.

6. Semchyshen, M. ; Barr, Robert Q. ; and Kalns, Eric: Development and Evaluation of Tungsten-Base Alloys. Final Rep. (Contract NOw-64-0057-C), Climax Molybdenum Co., Aug. 10, 1965. (Available from DDC as AD-468299).

7. Goldschmidt, H. J. ; and Brand, J. A. : Investigation Into the Tungsten-Rich Regions of the Binary Systems Tungsten-Carbon, Tungsten-Boron and Tungsten Beryllium. Part I - Tungsten-Carbon Equilibrium System. (AFASD-TDR-62-25, Pt. 1), B. S. A. Research Centre, Great Britain, Mar. 1962.

8. Giessen, Bill C. ; Rump, Irmgard; and Grant, Nicholas J. : The Constitution Diagram Tungsten-Hafnium. Trans. AIME, vol. 224, no. 1, Feb. 1962, pp. 60-64.

9. Stephens, J. R. : Dislocation Structures In Slightly Strained Tungsten, Tungsten-Rhenium, and Tungsten-Tantalum Alloys. Paper presented at the Fall Meeting AIME Chicago, Ill., 1966.

10. Keh, A. S. ; and Weissmann, S. : Deformation Substructure in Body-Centered Cubic Metals. Electron Microscopy and Strength of Crystals. Gareth Thomas and Jack Washburn, eds., Interscience Publishers, 1962, pp. 231-300.

11. Fine, Morris E. : Precipitate and Dispersion Hardening of Crystalline Solids. The Relation Between the Structure and Mechanical Properties of Metals. National Physical Laboratory Symposium No. 15, vol. 1. Her Majesty's Stationery Office (London), 1963, pp. 299-320.

12. Berghezan, A. ; and Fourdeux, A. : Deformation and Annealing Substructures of Niobium and Their Relation to the Mechanical Properties and Precipitation Phenomena. Symposium on the Role of Substructure in the Mechanical Behavior of Metals. I. Perlmutter, ed. , Rep. No. AFASD-TDR-63-324, Wright-Patterson AFB, Apr. 1963, pp. 437-476.

13. Gregory, Donald P. : Mechanisms of Work Hardening in Body Centered Cubic Metals. (AFASD-TDR-62-354, Pt. 111, AD-465709), Pratt and Whitney Aircraft, Mar. 1965.

14. Keh, A. S. ; Leslie, W. C. ; and Sponseller, D. L. : Interaction of Dislocations and Precipitates in Iron-Base Alloys. Precipitation from Iron-Base Alloys. Gilbert R. Speich and John B. Clark, eds. , Gordon and Breach Science Publishers, 1965, pp. 281-325.

15. Chang, W. H. : A Study of the Influence of Heat Treatment on Microstructure and Properties of Refractory Alloys. (AFASD-TDR-62-211), General Electric Co. , Apr. 1962.

16. Kelley, A. ; and Nicholson, R. B. : Precipitation Hardening. Vol. 10, No. 3 of Progress in Materials Science. The Macmillan Co., 1963.

17. Wilcox, B. A. ; and Clauer, A. H. : Steady-State Creep of Dispersion-Strengthened Metals. Battelle Memorial Inst. (NASA CR-54639), Aug. 19, 1966.

18. Ansell, G. S. ; and Weertman, J. : Creep of a Dispersion-Hardened Aluminum Alloy. Trans. AIME, vol. 215, no. 5, Oct. 1959, pp. 838-843.

19. Hirschhorn, J. S. ; and Ansell, G. S. : Dispersion Strengthening Models. Acta Met., vol. 13, no. 5, May 1965, pp. 572-573.

20. Bailey, J. E. : Electron Microscope Observations on Recovery and Recrystallization Processes in Cold-Worked Metals. Electron Microscopy and Strength of Crystals. Gareth Thomas and Jack Washburn, eds. , Interscience Publishers, 1962, pp. 535-574.

21. Hu, H. : Annealing of Silicon-Iron Single Crystals. Recovery and Recrystallization of Metals. L. Himmel, ed., Interscience Publishers, 1963, pp. 311-378.

NASA-Langley, 1968 — 17 E-3862